Multilevel Modulation Techniques for Millimeter Guided Waves

By W. M. HUBBARD, G. D. MANDEVILLE, and J. E. GOELL

(Manuscript received July 12, 1969)

This paper describes an investigation of the feasibility of increasing the information transmission capacity of a guided millimeter wave communication system by using quaternary and higher order modulation techniques in place of binary. It first presents a generalization of the binary system to higher orders and then extends the results of previously derived error-rate predictions. An experimental repeater for quaternary modulation which uses components that are similar to those used for binary modulation is then described along with associated equipment used for signal generation and performance evaluation. Finally, performance data on the repeater are given and compared with theory.

I. INTRODUCTION

The quaternary and higher-order modulation techniques which are described are extensions of the binary modulation technique previously discussed by the authors.[1] The earlier system uses binary differentially-coherent phase-shift-keyed (B-FMDCPSK) modulation, a form of modulation in which the frequency of the carrier is increased or decreased once during each time slot in such a manner that the phase (the time integral of the frequency shift) is changed by $\pm 90°$ relative to the phase of the previous time slot. Experimental repeaters were built which could regenerate, with a 10^{-9} error rate, a signal which had been attenuated by an amount equivalent to 15 miles of waveguide. In this repeater the incoming millimeter-wave signals from circular waveguide were passed through band- and channel-demultiplexing filters, down-converted, amplified, differentially phase-detected, and regenerated (utilizing timing information self-contained in the signal) to obtain a polar baseband representation of the information. This baseband signal was used to drive an IF voltage-tuned oscillator, the output of which was amplified, up-converted, passed through

channel- and band-multiplexing filters and launched into circular waveguide.

The modulation scheme of the system can be generalized in such a way that systems with $M = 2^m$ levels (quaternary, octonary, and so on) can be built with components most of which are the same as those used in the binary system. With such a system, the information capacity of the wave-guide can be increased by a factor m by using a 2^m level signal in each of the individual channels. The increase in system capacity is accompanied by a decrease in immunity to noise and system degradation (which is common to all multilevel systems) and a slight increase in system complexity.

A theoretical consideration of multilevel systems of all orders is given in Section II. This consideration amounts to an extension of previous error-rate calculations for binary systems.[2] Section III describes a quaternary (Q-FMDCPSK) system which has been built and operated at 320 megabits/s.

Because the theoretical portion of this paper is a direct extension of a previous paper on a binary system it is assumed that the reader is familiar with the contents of that paper.[2] However, references to the binary paper are made where appropriate as an aid to the reader.

II. THEORETICAL CONSIDERATION OF MULTILEVEL SYSTEMS

2.1 *Description of the Quaternary System*

The signal consists of a constant-amplitude angle-modulated carrier. The modulation is achieved by causing a frequency deviation once in each time slot. For the binary case the frequency deviation $\omega(t)$ satisfies the condition

$$\int_{(n-\frac{1}{2})T}^{(n+\frac{1}{2})T} \omega(t')\, dt' = \alpha_n \tag{1}$$

in the nth time slot, where $\alpha_n = \pm\pi/2$ and contains the binary information. This signal can be written in the form

$$s(t) = \cos\left[\omega_0 t + \int_0^t \omega(t')\, dt'\right] \tag{2}$$

where ω_0 is the center frequency about which the signal is deviated. Equations (1) and (2) hold for the quaternary signal as well. The only difference is that now α_n can take on any of the four values $\pm\pi/4, \pm 3\pi/4$.

The signal space diagrams of these signals are shown in Fig. 1. The states marked "×" represent the phase states which are available to

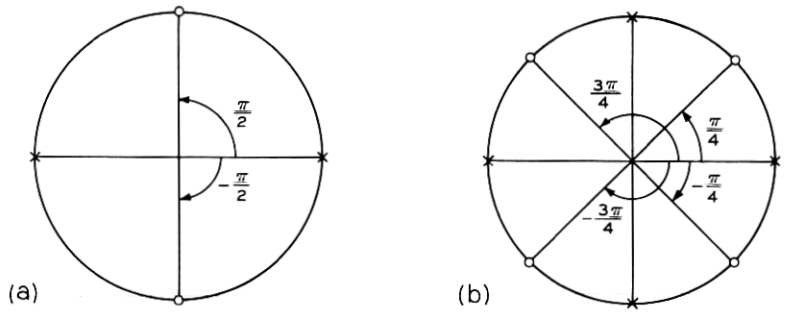

Fig. 1 — Signal space diagrams for DC phase-shift-keyed signals: (a) binary, (b) quaternary. × represents phase states available in even number time slots and "○" represents the phase states available in odd numbered time slots.

the signal in the even numbered time slots and those marked "○" represent the states which are available in odd numbered time slots. Thus the transition always takes place from a state marked × to a state marked ○ or vice versa.

Bennett and Davey describe the detection scheme for DCPSK modulation.[3] A particular embodiment of the differential phase detector for the binary signal of Fig. 1a is shown in Fig. 2. Here the relative delay between the two paths is T where T satisfies simultaneously the two constraints

$$\frac{1}{T} = \text{Baud rate}$$

$$\omega_0 T = (n + \tfrac{1}{2})\pi \quad n \text{ an integer.}$$

Figure 3 illustrates how this differential phase detection concept is

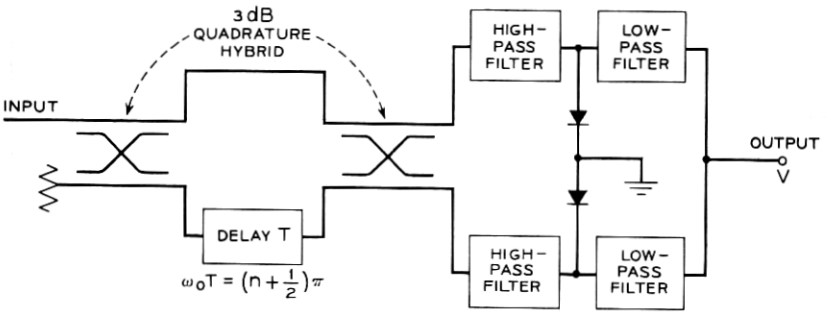

Fig. 2 — Binary differential phase detector.

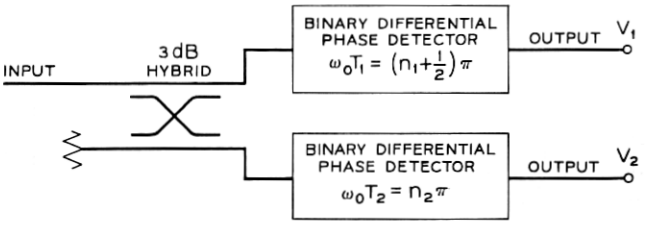

Fig. 3 — Quaternary differential phase detector.

extended to the quaternary case. In this case the preceding constraints become

$$\frac{1}{T_1} \approx \frac{1}{T_2} \approx \text{Baud rate}$$

$$\omega_0 T_1 = (n_1 + \tfrac{1}{2})\pi \qquad n_1 , n_2 \quad \text{integers.}$$

$$\omega_0 T_2 = n_2 \pi$$

If one applies the signal described by equations (1) and (2) to the device illustrated in Fig. 3, he finds that the outputs V_1 and V_2 are given by Table I for the four possible phase changes, α. Thus the binary variable V_1 defines the sign of α while V_2 defines its magnitude. Stated another way, given that the phase state in the $(n-1)$th time slot was at 0 radians in Fig. 1b, V_1 determines in which half plane (upper or lower) the phase state of the nth time slot lies while V_2 determines in which half plane (left or right) it lies.

Since each branch of the quaternary differential phase detector is identical to the binary device described in Ref. 2 the limiter and the regenerators can also be identical to those described in Sections III and 1.4 of Ref. 2.

For the multilevel system, only one device which is not a direct adaptation of an existing component of the binary system is required. Its function is to translate the regenerated binary signals into a signal

TABLE I — OUTPUTS FOR FOUR POSSIBLE PHASE CHANGES

α	V_1	V_2
$\pi/4$	1	1
$-\pi/4$	−1	1
$3\pi/4$	1	−1
$-3\pi/4$	−1	−1

suitable for driving the FM deviator. Its performance should be virtually error free and need not be considered in the error-rate calculations. A description of this translator is deferred to Section III.

2.2 *Extension of the Error-Rate Calculation*

The bit-error probability of the quaternary system described in Section 2.1 is equal to the probability that an error is made in one of the baseband binary sub-channels. This, however, is just the probability that an error is made in a binary differentially-coherent phase-shift-keyed system in which the expectation value of the second pulse is shifted an amount $\pi/4$ from where it should be for binary operation. (This phase shift from the desired binary-system value is represented by the quantity β_0 in Section III of Ref. 2.) The probability of bit error, Π can be restated for the quaternary case as*

$$\Pi = \tfrac{1}{2}P_0\left(\phi + \frac{\pi}{4} + \delta\right) + \tfrac{1}{2}P_0\left(\phi - \frac{\pi}{4} - \delta\right) \tag{3}$$

where

$$P_0(\Phi) = \frac{1}{2\pi}\int_{-\pi/2}^{\pi/2} \exp\left[-\frac{\cos^2\Phi}{2\sigma^2(1 + \sin\Phi\sin\theta)}\right] d\theta. \tag{4}$$

An approximate solution (in closed form) to this integral is derived in the Appendix. Here the quantities ϕ and δ have the same meaning as in Reference 2, namely, δ is the phase shift due to intersymbol interference and any other phase distortion in the system, and $\phi = \sin^{-1}\epsilon$ where ϵ is given by $S/T = -10\log\epsilon$† and S/T is the signal-to-threshold ratio of the regenerator in decibels. S/T is defined in Section 1.4 of Ref. 1 as the ratio of the expected value of signal power to the minimum value of signal power which will cause the regenerator to function realiably (in the absence of noise).

Values of P_0 for Φ from 0 to 30° are given in Ref. 2 for signal-to-noise ratios $S/N = 9$ through 15 dB. These results are extended in Fig. 4 to include values suitable for quaternary and higher level systems. Note that $P_0(\Phi)$ is even. Figure 5 shows error rate as a function of S/N for an ideal quaternary system.

The effects of finite S/T and δ are more pronounced for quaternary systems than for binary. The threshold effect noise figure N_T defined in Ref. 4 is shown in Fig. 6 for a quaternary system and for a binary

* Equations (3) and (4) follow directly from Equations (20) and (21) of Reference 2 by replacing δ with $\delta + \pi/4$.

† The equation relating S/T and ϵ in Ref. 2 is incorrect. The conclusions of Ref. 2 are not affected by this as the correct form of the relation was used in the calculations.

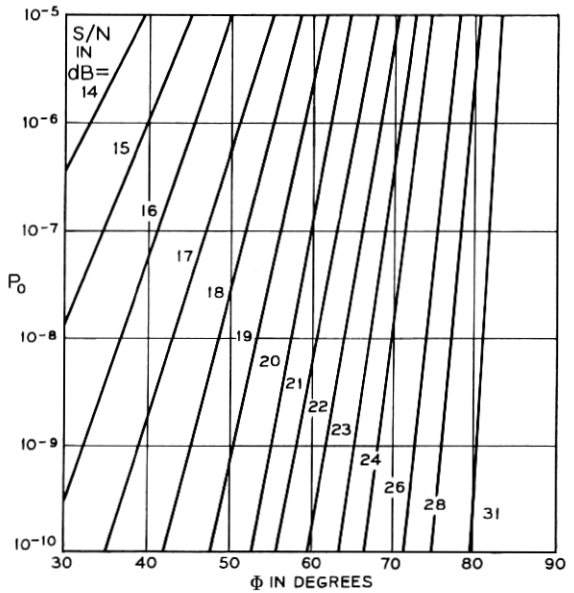

Fig. 4 — Error integral versus Φ for various values of S/N.

system. N_T is the amount by which S/N must be improved in order to offset the effect of a nonideal regenerator.

The effects of δ and S/T are determined directly from Fig. 7 which shows the value of S/N required for 10^{-9}, 10^{-8}, 10^{-6}, and 10^{-4} error-rate as a function of Φ. For comparison we consider the values of S/T and δ which were inferred from the measurements made on the binary repeater described in Ref. 1, namely $S/T = 10$ dB, $\delta = 10°$. For the binary case the combined effect of these degradations is about 0.8 dB whereas for the quaternary case the combined effect is about 3.4 dB. The theoretically predicted values* of S/N for operation with an error probability of 10^{-9} are therefore 13.8 dB and 21.3 dB for binary and quaternary, respectively (with half the bandwidth requirement in a quaternary system with the same bit rate). (The experimentally determined value for the binary system is 13.7 dB.)[1]

2.3 *Extension to Higher Level Systems*

In a system with 2^m levels, the signal described in Section 2.1 could be generalized to have 2^m equally spaced positions around the unit

* This value does not include degradation introduced into the quaternary system due to nonlinearity of the FM deviator. Unlike the binary case, this nonlinearity is important in the quaternary and higher order cases.

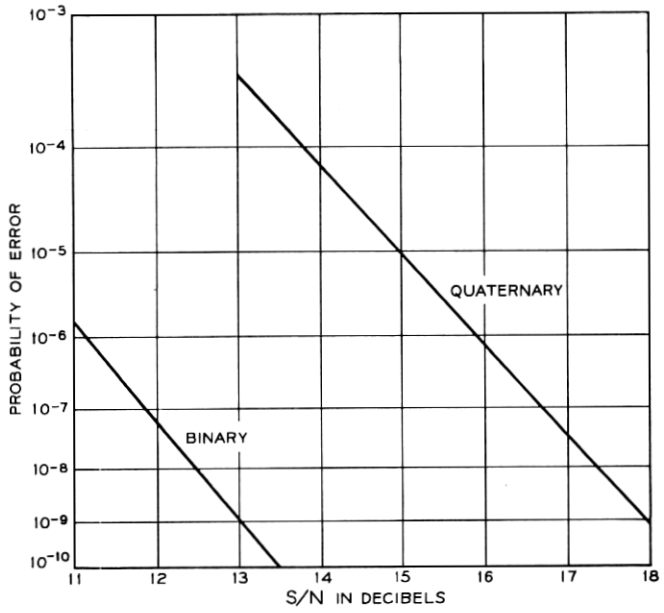

Fig. 5 — Probability of error in ideal binary and quaternary systems.

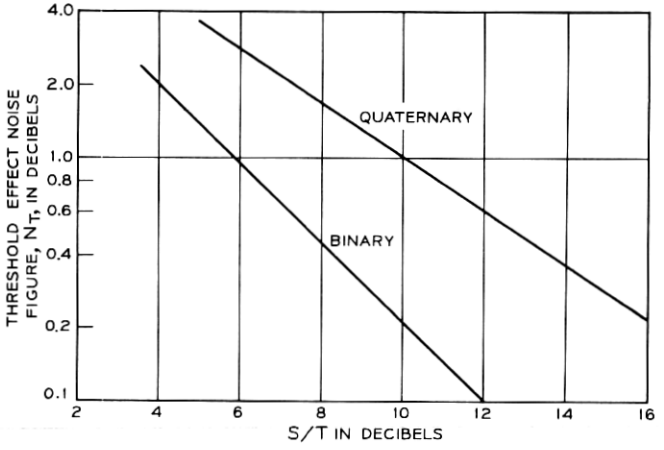

Fig. 6 — Threshold effect noise figures as a function of signal-to-threshold ratio, S/T.

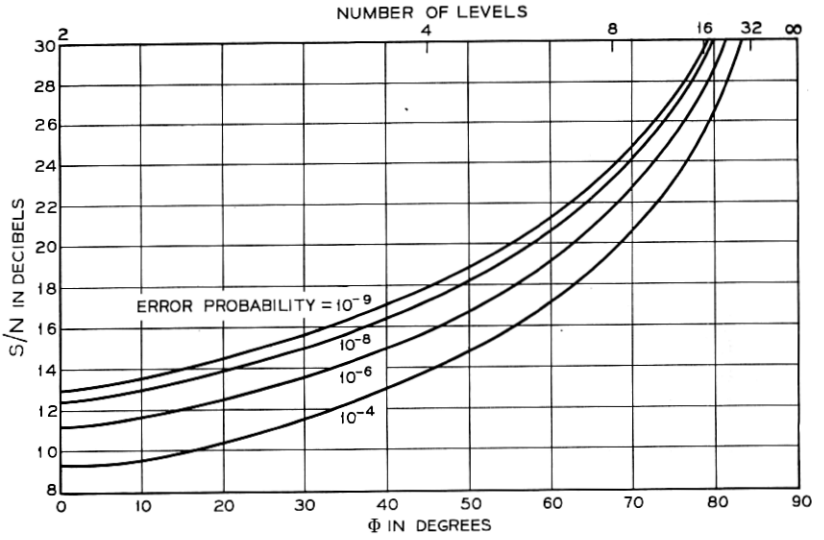

Fig. 7 — Required signal-to-noise ratio for various values of error probability as a function of Φ.

circle in the even numbered time slots. The differential phase detector would then require m of the binary differential phase detectors of Fig. 2, with delay lines T_1 , T_2 $\cdots$ T_m such that the values of $\omega_0 T_k$ are chosen to give 2^m equally spaced values around the unit circle beginning at $\pi/2^m$, that is,

$$\omega_0 T_k = \frac{(2k+1)\pi}{2^m}, \qquad k = 0, 1, \cdots, 2^m - 1.$$

In systems with more than four levels this method of detection gives more than one level of pulse height at the regenerator. The following consideration makes the approximation that the worst-case error-rate applies in all cases. This results in a calculated error-rate which is too large by a factor which is less than the ratio $M/(M-4)$ for an M level system ($M > 4$).

Equation (3) then becomes:

$$\Pi = \tfrac{1}{2}P_0\left(\phi + \delta + \frac{\pi}{2} - \frac{\pi}{M}\right) + \tfrac{1}{2}P_0\left(\phi - \delta - \frac{\pi}{2} + \frac{\pi}{M}\right) \qquad (5)$$

and equation (4) is unchanged. Figure 4 gives values of $P_0(\Phi)$ suitable for evaluating Π for values of M up to 16. Figure 7 indicates the values

of S/N required for 10^{-9}, 10^{-8}, 10^{-6} and 10^{-4} error-rate for ideal 2^m level systems for $m = 1$ through 5.

2.4 *Results of the Calculations*

In an ideal repeater the signal-to-noise ratio for an error rate of 10^{-9} is 13.0 and 17.9 dB for binary and quaternary signal, respectively. This amounts to a price of 4.9 dB for the doubling of the bit rate (or alternatively the halving of the bandwidth) achieved by quaternary systems. In an actual repeater with intersymbol interference and non-ideal regeneration comparable to that in the 306 megabits/s binary repeater of Ref. 1 there is an additional degradation of about 3.4 dB (compared with 0.8 dB for binary signals). Thus a signal-to-noise ratio of 21.3 dB is expected to be necessary for a 10^{-9} error rate in the quaternary repeater—a penalty of 7.5 dB compared with the binary repeater. For a guided-wave system of the sort described in Ref. 1 this requires only a 2.5 mile decrease in repeater spacing (about 10 to 15 percent) which might not be an unattractive price for doubling the channel capacity of the system.

For systems with more than four levels, the degradation in error-rate performance due to S/T and δ is even more severe. For eight levels ($m = 3$) for example, Φ becomes 83.2° (for the worst case) for $S/T = 10$ dB and $\delta = 10°$ and the degradation is (from Fig. 4) intolerable. Clearly an improvement in S/T and a substantial improvement in δ is necessary in order to make systems with more than four levels feasible. Even for ideal systems ($S/T = \infty$, $\delta = 0$), signal-to-noise ratios of about 23.7 dB and 29.7 dB are required for 10^{-9} error-rate for eight and sixteen level systems respectively compared with 13.0 dB and 17.9 dB for two and four level systems.

III. EXPERIMENTAL RESULTS FOR QUATERNARY REPEATERS

3.1 *Description of the Experimental Repeater*

The quaternary experimental system, shown in Fig. 8 is similar to the binary system described in Ref. 1 with the following exceptions.

(*i*) Where one differential phase detector and one regenerator were used in the binary, two are required. In addition, a binary device called a translator is needed.

(*ii*) Conversion into and out of the millimeter medium was omitted.

(*iii*) Modulation of a deviator by the regenerated baseband signal was not attempted.*

* The technique for doing this, however, is identical to the technique used to synthesize the signal from the random word generator and should present no additional problems.

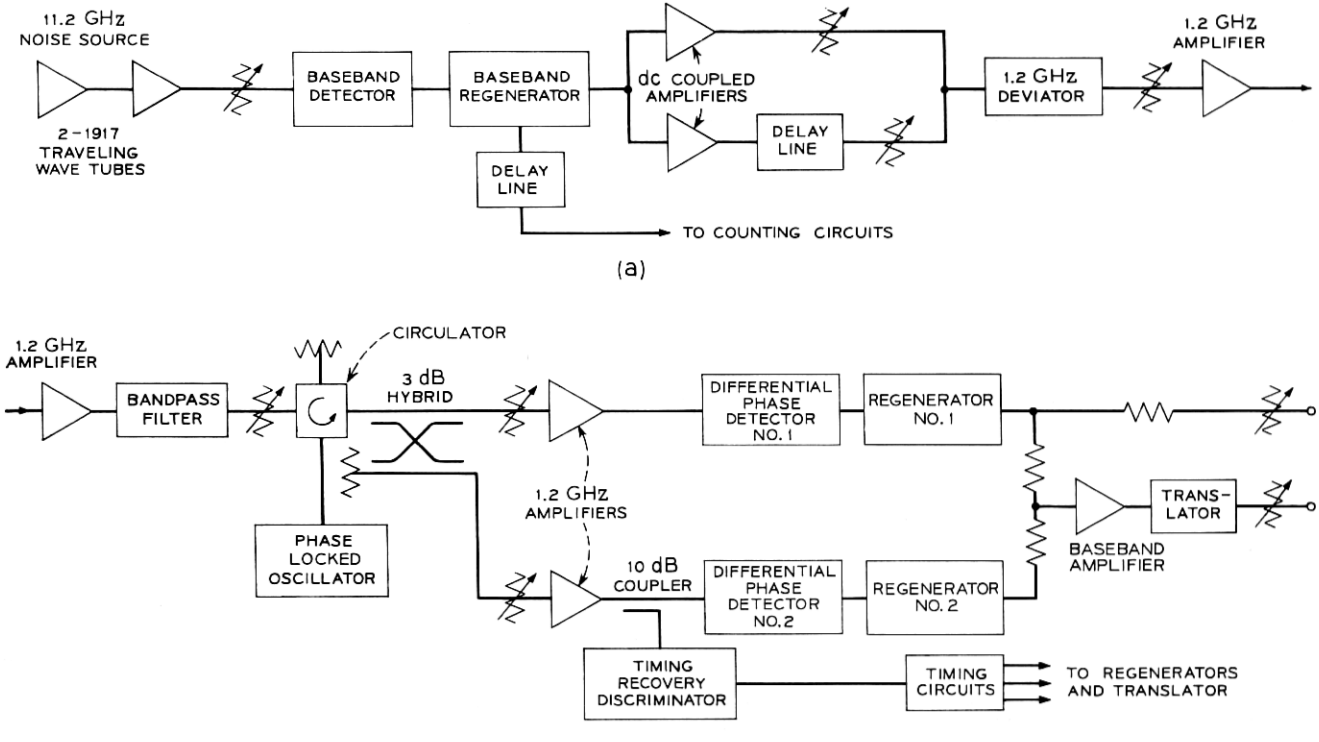

Fig. 8 — Block diagram of quaternary experiment. (a) Transmitter (word generator and IF phase modulator) and (b) Receiver (IF amplifier; limiter, phase detector, and regenerator).

(*iv*) A symbol (baud) rate of 160 MHz (320 megabits/s) was used.

In a quaternary FM phase-shift-keyed (Q-FMDCPSK) signal the information is contained in the phase shift between adjacent time slots. The phase shifts used are $\pm 3\pi/4$ and $\pm \pi/4$. The signal is generated by a voltage-controlled oscillator whose frequency is pulsed between sampling instants so that the time integral of the frequency shift is equal to the desired phase shift. An illustration of such a signal is shown in Fig. 9.

A four-level baseband pulse train is derived from a two-level polar source identical to the one used for the binary experiment[1] except for the rate which in the quaternary experiment was chosen to be 160 MHz. The random binary output signal is divided into two signals. One of the signals is delayed a few integral time slots and the other is attenuated 6 dB. They are then recombined. The combination of $+2$, -2 with $+1$, -1 pulses produces a pulse of one of four levels in each time slot (see Fig. 10a). These are $+3$, $+1$, -1, and -3, which produce phase shifts in the deviator $3\pi/4$, $\pi/4$, $-\pi/4$, and $-3\pi/4$, respectively. By delaying one signal a few time intervals, we closely approximate the effect of two independently random binary signals and thus obtain a virtually random four-level signal. Observation of the spectrum displayed by a spectrum analyzer verifies the randomness (see Fig. 10d).

Identifying the larger binary component as signal #1 and the smaller as signal #2 will help clarify the explanation of the regeneration process which follows. For the binary system, the signal was detected by a differential phase detector, the output of which is given by

$$\cos [\phi(t) - \phi(t - \tau) + \omega_0 \tau]$$

where ϕ is the phase angle of the signal, τ is the time delay introduced by a delay line built into the device, and ω_0 is the angular carrier frequency. For the binary case, τ was made equal to the bit interval and $\omega_0 \tau$ equal to $\pi/2 + n\pi$. The operation of the differential phase detector is illustrated in Fig. 11. The reference phase is taken as the phase of the signal in the previous time slot. The information given by the device is the projection E_v of the signal S along the vertical axis. The two phase transitions of the binary case, $\pm \pi/2$, are fully determined by the sign of E_v.

For a quaternary signal, it is not possible to distinguish between transition into regions I and II or those into III and IV using only E_v. This problem was solved by splitting the IF signal into two portions, one of which was connected to a differential phase detector with $\tau = T_1$

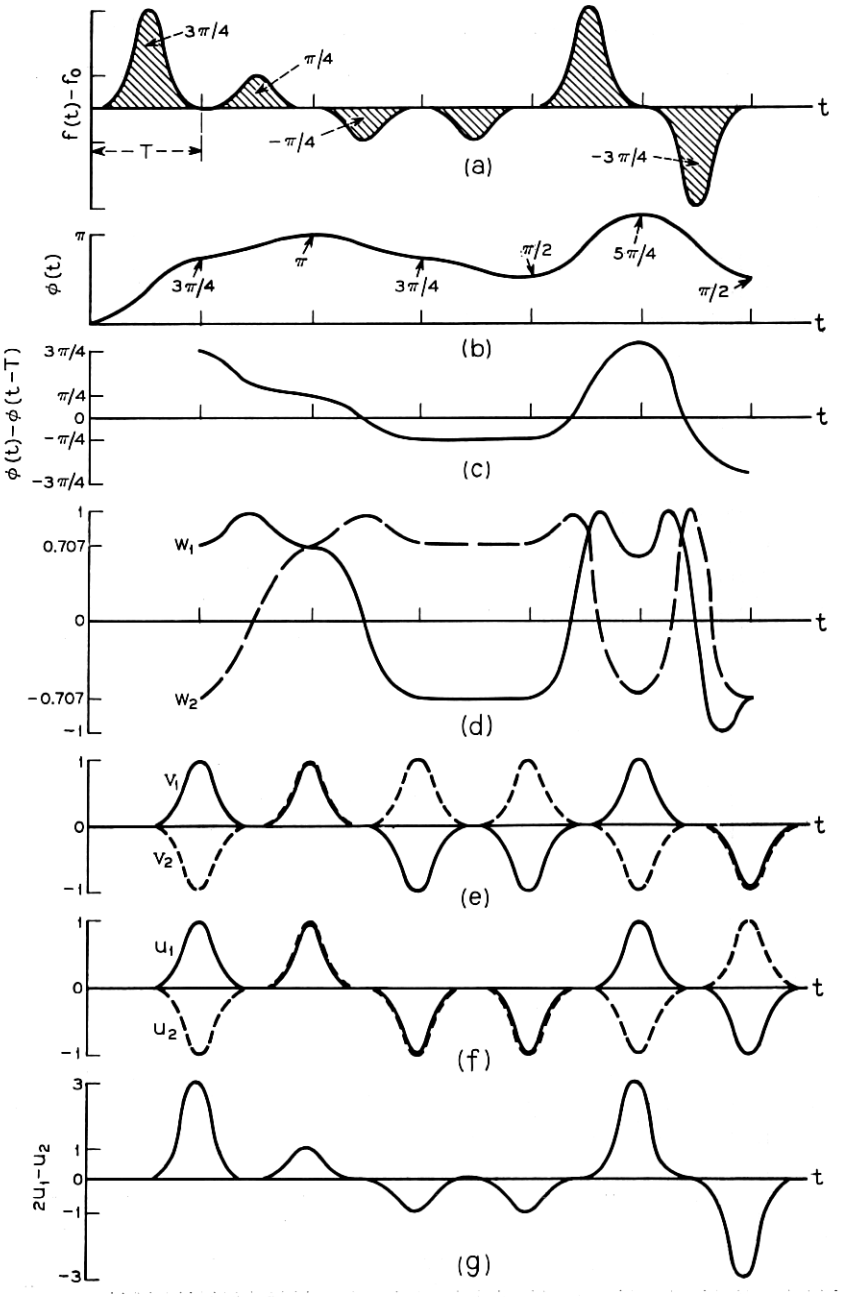

Fig. 9 — Representative quaternary frequency-modulation differentially-coherent phase-shift-keyed signal.

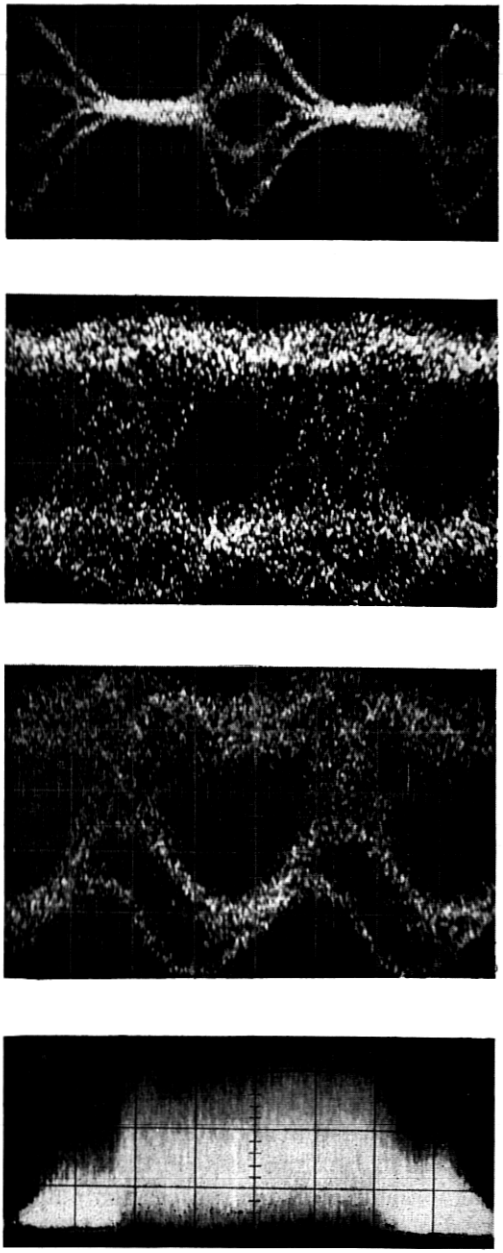

Fig. 10 — (a) Random four-level base-band pulses ($H = 2$ ns/cm); (b) symmetric eye ($H = 2$ ns/cm); (c) asymmetric eye ($H = 2$ ns/cm); and (d) IF spectrum ($H = 30$ MHz/cm).

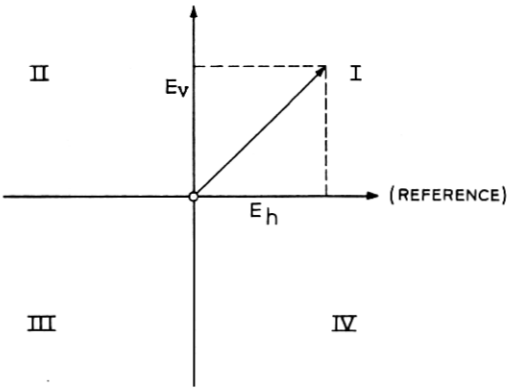

Fig. 11 — Operation of the differential phase detector.

and the other was connected to a differential phase detector with $\tau = T_2$. The quantities ω_0 , T_1 , and T_2 were chosen so that

$$\omega_0 T_1 = 16.5\pi \quad \text{and} \quad \omega_0 T_2 = 16\pi$$

in order to satisfy the conditions set forth in Section II. Thus the output of the first differential phase detector gives E_v , and the output of the second E_h . From the signs of E_h and E_v the quadrant of the signal can be determined as shown in Table II. Figures 10(b) and (c) are photographs of sampling oscilloscope displays of the two phase-detector outputs of a typical random signal. Because signal state #2 does not correspond to either E_v or E_h a translator is required. If E_h and E_v are regenerated so that they have unit magnitude, then signal #1 is given by E_v and signal #2 is given by the negative of the product, E_vE_h . The sign of the product E_vE_h was determined by the translator circuit shown in Fig. 12. This circuit is similar to the balanced-line logic element used in the binary regenerators except for the input circuit; it functions as follows. Without input, once each time slot either diode A or diode B must switch into its high-voltage state while the other diode remains in its low-voltage state. Applying positive bias causes diode B to switch giving positive output pulses while applying negative bias produces the opposite effect. For the translator circuit the bias is set so that diode B always switches into the high-voltage state in the absence of input. The input to the circuit is the sum of the regenerated outputs of the two differential phase detectors E_v and E_h . If the sum of the two signals is zero, diode B switches so the output pulse is positive. If the sum of the two signals is either positive or negative diode A switches and a

TABLE II — DETERMINATION OF THE QUADRANT OF THE SIGNAL

Quadrant	Phase Shift at Transmitter	E_v	E_h	Original Signal #1	Original Signal #2
I	$\pi/4$	+	+	+	−
II	$3\pi/4$	+	−	+	+
III	$-3\pi/4$	−	−	−	−
IV	$-\pi/4$	−	+	−	+

negative output results, since for either polarity, current flowing through the steering diodes, D_1 and D_2 , increases the current through diode B. Thus the translator output is equivalent to the product of the regenerated E_v and E_h signals.

3.2 *Results*

The error rate was measured as in the binary experiment, except that the two binary components of the regenerated quaternary baseband signal were compared separately with their properly delayed counterparts comprising the input baseband signal.

The results of the error-rate measurements are shown in Fig. 13. Curve 1 shows the error-rate performance which was obtained when the equipment was originally built. At high error-rates (above about 5×10^{-6}) the performance was in good agreement with the theoretical

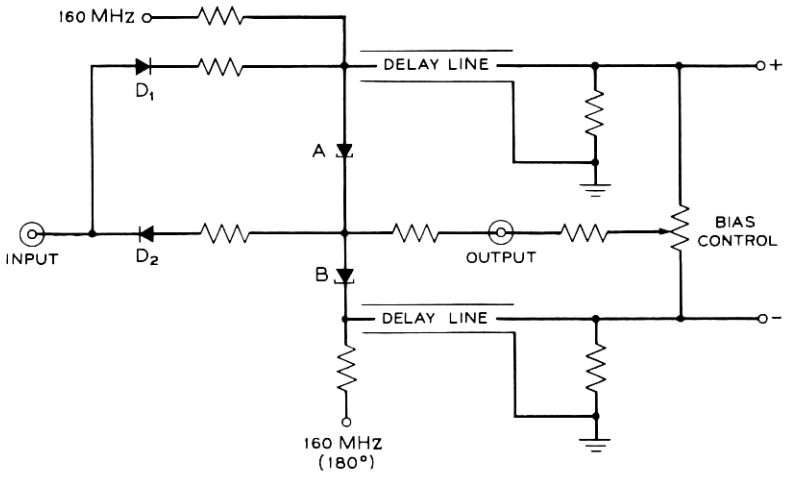

Fig. 12 — Schematic of translator circuit.

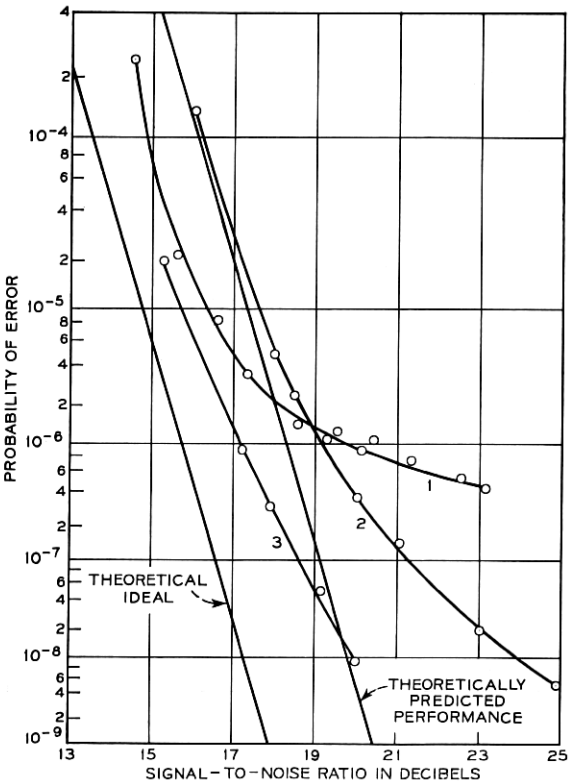

Fig. 13 — Results of error-rate measurements.

predictions. There was, however, a "floor" at an error-rate of about 4×10^{-7} and no increase in the S/N would reduce the error-rate below this value. It should be noted that the degradations considered in Section II shift the error-rate line to larger S/N and decrease the slope slightly (in magnitude) but do not tend to establish a "floor" such as the one shown by curve 1. It might also be mentioned that a "floor" similar to this is characteristic of experimental error-rate curves for the binary repeater of Ref. 1, but there it occurred typically at error-rates below 10^{-10} and was therefore considered insignificant.

Thus the indication was that the "floor" was the result of some degradation which was neglected in the theory and to which the four-level system was far more sensitive than was the two-level system. One possibility was that the impairment was due to slight mismatches

among the commercial components. Improved performance was achieved by careful selection of components with particular emphasis on the linearity of the deviator. Curves 2 and 3 of Fig. 13 show the typical and best performance, respectively. The "floor" was at 8×10^{-10} when curve 3 was observed. Thus the agreement between theory and experiment is fairly good at error-rates substantially above the experimentally observed floor.

3.3 *Conclusions*

The quaternary experiment was restricted to the investigation of the modulation and regeneration aspects of a repeater system. However, the data obtained, coupled with the results from the previous binary experiment, suggest that a quaternary (Q-FMDCPSK) repeater system is feasible and might have applications where the conservation of bandwidth is desirable and the cost in terms of noise immunity can be afforded. Systems with eight or more levels do not seem feasible at the present time.

APPENDIX

Evaluation of the Error-Rate Integral

The integral $P_0(\Phi)$ [equation (4)] or its equivalent

$$P_0 = \frac{1}{2\pi} \int_{-\infty}^{\infty} \int_{-\infty}^{\infty} \exp\left[-(x - p_x)^2 - (y - p_y)^2\right] \cdot \operatorname{erfc}\left[\frac{xq_x + yq_y}{(x^2 + y^2)^{\frac{1}{2}}}\right] dx\, dy \qquad (6)$$

is frequently encountered in error-rate calculations for digital phase and frequency modulated signals.[1,2,4,5] The equivalence of these two forms can be shown by arguments similar to those of Ref. 5. Namely, the integral in the form of equation (6) is written in polar coordinates and the integration over r is performed to give

$$P_0 = \frac{1}{2\pi} \int_0^{2\pi} \exp(-p^2 \sin^2 \phi) \operatorname{erfc}[q \cos(\phi + \gamma)] \cdot \left[\tfrac{1}{2} \exp(-p^2 \cos^2 \phi) + p \cos\phi \frac{\pi^{\frac{1}{2}}}{2} \operatorname{erfc}(-p \cos\phi)\right] d\phi$$

where

$$p = (p_x^2 + p_y^2)^{\frac{1}{2}}, \qquad \gamma = \operatorname{atn} \frac{q_y}{q_x} - \operatorname{atn} \frac{p_y}{p_x}, \qquad q = (q_x^2 + q_y^2)^{\frac{1}{2}}.$$

This integral can be greatly simplified by writing the error function compliments in terms of their respective error functions and making use of the odd parity of the error function. When this is done the only nonvanishing terms are (after some simplification)

$$P_0 = \frac{1}{2} - \frac{1}{\pi}\int_{-p}^{p}\int_{0}^{(p/q)[(p^2-x^2)^{\frac{1}{2}}\cos\gamma - x\sin\gamma]} \exp(-x^2 - y^2)\,dx\,dy. \quad (7)$$

The limits of integration in equation (7) form half of an ellipse. Because of the spherical symmetry of the integrand we can pick any half of this ellipse. Thus the integral can be written

$$P_0 = \frac{1}{2\pi}\int_{-\pi/2}^{\pi/2}\int_{0}^{R(\phi)} \exp(-r^2) r\,dr\,d\phi$$

where (after some simplification) one finds

$$R(\phi) = \left[\frac{S\cos^2\Phi}{1 + \sin\Phi\sin 2\phi}\right]^{\frac{1}{2}}$$

and

$$S = \frac{p^2 + q^2}{2} \qquad \cos\Phi = 2\frac{qp\cos\gamma}{p^2 + q^2}.$$

Performing the radial integration gives

$$P_0(\Phi) = \frac{1}{2\pi}\int_{-\pi/2}^{\pi/2} \exp\left(-\frac{S\cos^2\Phi}{1 + \sin\Phi\sin\theta}\right) d\theta$$

which is equation (4) with the substitution

$$S = \frac{1}{2\sigma^2}.$$

As a first step in finding an approximate solution to $P_0(\Phi)$ we can write

$$P(\Phi) = \frac{1}{2\pi}\int_{-\pi/2}^{\pi/2} \exp[-S\cos^2\Phi(1 - \sin\Phi\sin\theta)]\,d\theta.$$

But $P(\Phi)$ can be integrated to give

$$P(\Phi) = \tfrac{1}{2}\exp(-S\cos^2\Phi) I_0(S\cos^2\Phi\sin\Phi)$$

where I_0 is the modified Bessel Function of the first kind. Now $P(\Phi)$ must be a good approximation to $P_0(\Phi)$ for sufficiently small Φ. In fact, for $\Phi = 0$ and $\Phi = \pm\pi/2$ we have

$$P(0) = P_0(0) = \tfrac{1}{2}\exp(-S)$$

and

$$P\left(\pm\frac{\pi}{2}\right) = P_0\left(\pm\frac{\pi}{2}\right) = \tfrac{1}{2},$$

respectively. Thus $P(\phi)$ and $P_0(\phi)$ agree at both extremes.

Let $g(P)$ be the integrand of the integral for P and $g(P_0)$ the integrand of that for P_0 . Their ratio is

$$R(\Phi, \theta) = \frac{g(P)}{g(P_0)} = \exp\left\{\frac{S}{4}\cdot\frac{\sin^2(2\Phi)\sin^2\theta}{1+\sin\Phi\sin\theta}\right\}.$$

We observe that $R \geqq 1$ everywhere. In the following argument we assume for clarity that $\Phi > 0$; but it can easily be verified that similar arguments can be constructed for the case $\Phi < 0$ and the same results obtained.

$R(\Phi, \theta)$ has an absolute maximum R_{AM} at $\theta = -\pi/2$ and a relative maximum R_{RM} at $\theta = \pi/2$

$$R_{AM} = \exp\left\{\frac{S}{4}\cdot\frac{\sin^2 2\Phi}{1-|\sin\Phi|}\right\}$$

$$R_{RM} = \exp\left\{\frac{S}{4}\cdot\frac{\sin^2 2\Phi}{1+|\sin\Phi|}\right\}.$$

Thus we have rigorous bounds

$$P(\Phi) \geqq P_0(\Phi) \geqq P(\Phi)/R_{AM} .$$

Unfortunately these bounds are often too loose to be of much value.

Inspection of the integral for P_0 reveals, however, that almost none of the contribution to the integral comes from the region near $\theta = -\pi/2$ and in fact almost all of the contribution comes from the region near $\theta = \pi/2$ where $R(\Phi, \theta) \approx R_{RM}$. This suggests that we consider the expression

$$\begin{aligned} P_1(\Phi) &= P(\Phi)/R_{RM} \\ &= \tfrac{1}{2}\exp\left\{-S\left(1-\sin^3\Phi\right)\right\} I_0(S\cos^2\Phi\sin\Phi) \end{aligned}$$

as an approximation to $P_0(\Phi)$. Note that $P_1(\Phi)$ also possesses the property that

$$P_1(0) = P_0(0), \qquad P_1(\pm\pi/2) = P_0(\pm\pi/2).$$

Finally, one finds empirically that a somewhat better approximation is given by

$$P_2(\Phi) = P_1(\Phi)[1 + \tfrac{1}{2}|\sin(2\Phi)|].$$

It has been verified by numerical calculations of P_0 that for values of S and ϕ which give $10^{-11} < P_0 < 10^{-3}$ the accuracy of the approximation is better than 10 percent for $\Phi < 50°$ and remains better than 36 percent up to $\Phi = 80°$. In this range of error rates a variation of 40 percent in P corresponds to a variation of a few tenths of a decible in S/N. This form is most useful for binary systems (Φ small) even though it is valid for a wide range of values of Φ; a simpler form is derived below which is valid for large Φ and is therefore more convenient for quaternary and higher order systems.

It has been pointed out by H. O. Pollak that the integral

$$\int_s^\infty \exp(-x) I_0(x \sin \Phi)\, dx$$

which arises from consideration of a sine wave plus random noise[6] is closely related to the error-rate integral $P_0(\Phi)$. Pollak's proof is sketched below.

Set

$$p = S \cos^2 \Phi, \qquad \alpha = \sin \Phi,$$

$$y = \frac{-1}{1+\alpha} + \frac{1}{1+\alpha \sin \theta}, \qquad b = \frac{\alpha}{1-\alpha^2}.$$

Then equation (4) becomes (after some simplification)

$$P_0 = \frac{\exp\left(\frac{-p}{1+\alpha}\right)}{2\pi(1-\alpha^2)^{\frac{1}{2}}} \int_0^{2b} \frac{\exp(-py)\, dy}{\left(y + \frac{1}{1+\alpha}\right)(2by - y^2)^{\frac{1}{2}}}.$$

But[7]

$$\int_0^{2b} \frac{\exp(-py)}{(2by - y^2)^{\frac{1}{2}}}\, dy = \pi \exp(-bp) I_0(bp)$$

from which it can readily be shown that

$$P_0 = \frac{\cos \Phi}{2} \int_s^\infty \exp(-x) I_0(x \sin \Phi)\, dx.$$

From this form of the error-rate integral an approximate solution can be derived when $S \sin \Phi$ is sufficiently large to expand the Bessel Function as*

$$I_0(z) = \frac{\exp(z)}{(2\pi z)^{\frac{1}{2}}}.$$

* For $|z| > 0.15$ this approximation is valid to within 17 percent.

TABLE III—S/N INCREASE FOR VARIOUS NUMBERS OF LEVELS

Number of levels	Approximate increase in S/N in dB from the binary coherent phase-shift-keyed case for same error-rate
2	0.5
4	5.3
8	11.2
16	17.2
32	23.2
and so on	and so on

Making this substitution and performing the integration gives

$$P_0 = \frac{1}{2}\left[\frac{1 + |\csc \Phi|}{2}\right]^{\frac{1}{2}} \operatorname{erfc}\{[(1 - |\sin \Phi|)S]^{\frac{1}{2}}\}.$$

When both $|\sin \Phi| > 0.15$ and $|\sin \Phi| > 0.15/S$ hold, this can be written, to an accuracy of a factor of two, as simply

$$P_0 = \tfrac{1}{2} \operatorname{erfc}\{[(1 - |\sin \Phi|)S^{\frac{1}{2}}\}.$$

For cases of interest for quaternary and higher order systems these constraints are well satisfied and this approximation is very good.

For the M-level case with $\delta = \phi = 0$, (no phase distortion)

$$\Pi = \tfrac{1}{2} \operatorname{erfc}\left[\left\{\left[1 - \sin\left(\frac{\pi}{2} - \frac{\pi}{M}\right)\right]S\right\}^{\frac{1}{2}}\right]$$

$$= \tfrac{1}{2} \operatorname{erfc}\left\{\left[4\left(\sin^2 \frac{\pi}{2M}\right)S\right]^{\frac{1}{2}}\right\}.$$

For large M this becomes

$$\Pi = \tfrac{1}{2} \operatorname{erfc}\left(\frac{\pi}{M} S^{\frac{1}{2}}\right).$$

Thus, the S/N must be increased by 6 dB each time the number of levels is doubled if the error-rate is to remain constant. This is illustrated in Table III.

REFERENCES

1. Hubbard, W. M., Goell, J. E., Warters, W. D., Standley, R. D., Mandeville, G. D., Lee, T. P., Shaw, R. C., and Clouser, P. L., "A Solid-State Regenerative Repeater for Guided Millimeter-Wave Communication Systems," B.S.T.J., *46*, No. 9 (November 1967), pp. 1977–2018.
2. Hubbard, W. M., "The Effect of Intersymbol Interference on Error-Rate in Binary Differentially-Coherent Phase-Shift-Keyed Systems," B.S.T.J., *46*, No. 6 (July–August 1967), pp. 1149–1172.

3. Bennett, W. R., and Davey, J. R., *Data Transmission,* New York: McGraw-Hill, 1965.
4. Hubbard, W. M., "The Effect of a Finite Width Decision Threshold for Binary Differentially-Coherent PSK System," B.S.T.J., *45,* No. 2 (February 1966), pp. 307–319.
5. Bennett, W. R., and Salz, J., "Binary Data Transmission by FM Over a Real Channel," B.S.T.J., *42,* No. 5 (September 1963), p. 2387,
6. Rice, S. O., "Statistical Properties of a Sine Wave Plus Noise," B.S.T.J., *27,* No. 1 (January 1948), pp. 109–157.
7. Erdelyi, A., editor, *Tables of Integral Transforms,* vol. 1, New York: McGraw-Hill, 1953, p. 138 (14).